

# A numerical study of transport and shot noise in 2D hopping

Yusuf A Kinkhabwala<sup>1</sup>, Viktor A Sverdlov<sup>1</sup>, Alexander N Korotkov<sup>2</sup> and Konstantin K Likharev<sup>1</sup>

<sup>1</sup> Department of Physics and Astronomy, Stony Brook University, Stony Brook, NY 11794-3800, USA

<sup>2</sup> Department of Electrical Engineering, University of California-Riverside, Riverside, CA 92521, USA

Received 8 July 2005, in final form 12 October 2005

Published 27 January 2006

Online at [stacks.iop.org/JPhysCM/18/1999](http://stacks.iop.org/JPhysCM/18/1999)

## Abstract

We have used modern supercomputer facilities to carry out extensive Monte Carlo simulations of 2D hopping (at negligible Coulomb interaction) in conductors with a completely random distribution of localized sites in both space and energy, within a broad range of the applied electric field  $E$  and temperature  $T$ , both within and beyond the variable-range hopping region. The calculated properties include not only dc current and statistics of localized site occupation and hop lengths, but also the current fluctuation spectrum. Within the calculation accuracy, the model does not exhibit  $1/f$  noise, so that the low-frequency noise at low temperatures may be characterized by the Fano factor  $F$ . For sufficiently large samples,  $F$  scales with conductor length  $L$  as  $(L_c/L)^\alpha$ , where  $\alpha = 0.76 \pm 0.08 < 1$ , and parameter  $L_c$  is interpreted as the average percolation cluster length. At relatively low  $E$ , the electric field dependence of parameter  $L_c$  is compatible with the law  $L_c \propto E^{-0.911}$  which follows from directed percolation theory arguments.

## 1. Introduction

The theory of hopping transport in disordered conductors [1–3] at negligible Coulomb interaction is often perceived as a well established (if not completed) field, with recent research focused mostly on Coulomb effects. However, only relatively recently was it recognized that shot noise (see, e.g., [4]) is a very important characteristic of electron transport. In particular, the suppression of the current fluctuation density  $S_I(f)$  at low frequencies, relative to its Schottky formula value  $2e\langle I \rangle$  (where  $\langle I \rangle$  is the dc current), is a necessary condition [5] for the so-called quasi-continuous ('sub-electron') charge transfer in such finite-current experiments as single-electron oscillations [6].

Earlier calculations of shot noise at hopping through very short samples (e.g., across thin films [7, 8]) and simple lattice models of long conductors in 1D [9] and 2D [10] have shown

that such suppression may, indeed, take place. However, calculations for the more realistic case of disordered 2D conductors have been limited to just one particular value of electric field [10]. It seemed important to examine whether the law governing this suppression is really as general as it seemed. Such examination, carried out in this work, has become practical only since the development of a new, advanced method of spectral density calculation [11] in combination with the use of modern supercomputers. (The work reported below took close to a million processor-hours of CPU time.)

As a useful by-product of this effort, we have obtained accurate quantitative characterization of not only the dependence of the average current on both temperature  $T$  and electric field  $E$ , but also the statistics of localized site occupation and hop lengths, which give a useful additional insight into the physics of hopping transport.

## 2. Model

We have studied hopping in 2D rectangular ( $L \times W$ ) samples with ‘open’ boundary conditions on the interface with well conducting electrodes [10]—see the inset in figure 1. In the present study, we have concentrated on broad samples with width  $W \gg L_c$ , where  $L_c$  is the effective percolation cluster size (see below). The conductor is assumed to be ‘fully frustrated’: the localized sites are randomly distributed over the sample area, and the corresponding electron eigenenergies  $\varepsilon_j^{(0)}$  are randomly distributed over a sufficiently broad energy band, so that the 2D density of states  $\nu_0$  is constant at all energies relevant for conduction. Electrons can hop from any site  $j$  to any other site  $k$  with the rate

$$\gamma_{jk} = \Gamma_{jk} \exp\left(-\frac{r_{jk}}{a}\right), \quad (1)$$

where  $r_{jk} \equiv \sqrt{(x_j - x_k)^2 + (y_j - y_k)^2}$  is the site separation distance, and  $a$  is the localization radius<sup>3</sup>. Such exponential dependence on the hop length has been assumed in virtually all theoretical studies of hopping. (The corrections to this law due to phase interference effects [12–14] are typically small.) However, in contrast to most other authors, we take equation (1) literally even at small distances  $r_{jk} \sim a$ ; this range is important only at very high fields and/or temperatures where the average value of  $r_{jk}$  becomes comparable to  $a$ . Of course our quantitative results for this particular region are only true for the localized states with exponential wavefunction decay.

Another distinction from some other works in this field is that we assume that the hopping rate amplitude  $\Gamma_{jk}$  depends continuously on the localized site energy difference  $\Delta U_{jk} \equiv \varepsilon_j^{(0)} - \varepsilon_k^{(0)} + e\mathbf{E}\mathbf{r}_{jk}$ :

$$\hbar\Gamma_{jk}(\Delta U_{jk}) = g \frac{\Delta U_{jk}}{1 - \exp(-\Delta U_{jk}/k_B T)}. \quad (2)$$

This model coincides, for low phonon energies  $\Delta U_{jk}$ , with that described by equations (4.2.17)–(4.2.19) of [2] for hopping in lightly doped semiconductors, and of course satisfies the Gibbs detailed balance requirement  $\Gamma_{jk} = \Gamma_{kj} \exp(\Delta U_{jk}/k_B T)$ . It is also close to, but more physical than, the ‘Metropolis’ dependence, which has a cusp at  $\Delta U_{jk} = 0$ .

The interaction of hopping electrons is assumed negligible (with the exception of their implicit on-site interaction, which forbids hopping into already occupied localized states). This assumption is well justified for practically important materials, in particular very thin films of amorphous silicon, which is the major candidate material for the implementation

<sup>3</sup> Note that in contrast with some prior publications, we do not include the factor 2 in the exponent. This difference should be kept in mind at the result comparison.

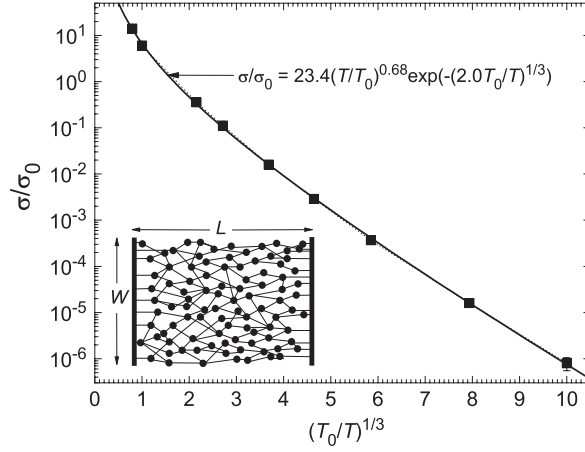


**Figure 1.** Linear conductivity  $\sigma$  as a function of temperature  $T$ . Points show the results of averaging over 80 samples varying in size ( $L \times W$ ) from  $(20 \times 10)a^2$  to  $(160 \times 100)a^2$ , biased by a low electric field  $E \ll E_T$ . Points are Monte Carlo results. The thin dashed line is just a guide for the eye, while the thick solid line corresponds to the best fit of the data by equation (5). Here and below, the error bars are smaller than the point size, unless they are shown explicitly. (The error bars correspond to the uncertainty in averaging over an ensemble of independent samples that is larger than the calculational uncertainty for each of the samples.) The inset shows the system under analysis (schematically).

of sub-electron charge transfer components in single-electronic circuits [15]. Indeed, the relative strength of the Coulomb interaction may be characterized by a dimensionless parameter  $\chi \equiv (e^2/\kappa a) \times (v_0 a^2)$ , where  $\kappa$  is the relative dielectric constant [16]. For a film of thickness  $t \sim a$ ,  $v_0$  may be estimated as  $t\nu$ , where  $\nu$  is the 3D density of states. For undoped amorphous Si,  $\nu$  is of the order of  $10^{16} \text{ eV}^{-1} \text{ cm}^{-3}$ , and only special treatments may increase it to  $\sim 10^{20} \text{ eV}^{-1} \text{ cm}^{-3}$ —see, e.g., [17]. As a result, for  $\kappa \sim 10$  and  $a \sim 3 \text{ nm}$  (both numbers are typical for the midgap states in Si),  $\chi$  is much less than unity for the entire range of  $\nu$  cited above, so that there is a broad range ( $\Delta(\ln T), \Delta(\ln E) \sim 3 \ln(\chi^{-1})$ ) of temperature  $T$  and electric field  $E$  where the Coulomb interaction is negligible [16].

With this assumption, our model has only three energy scales:  $k_B T$ ,  $eEa$ , and  $(v_0 a^2)^{-1}$ . In other words, there are two characteristic values of electric field:

$$E_T \equiv \frac{k_B T}{ea} \quad \text{and} \quad E_0 \equiv \frac{1}{e v_0 a^3}. \quad (3)$$

We will be mostly interested in the case of low temperatures  $T < T_0$ , where

$$T_0 \equiv \frac{1}{k_B v_0 a^2} \quad (4)$$

is the field-independent scale of temperature, so that the field scales are related as  $E_T < E_0$ . (The only role of the dimensionless parameter  $g$  introduced by equation (2) is to give the scale of hopping conductivity  $\sigma_0 \equiv g(e^2/\hbar)$ . Coherent quantum effects leading to weak localization and metal-to-insulator transition are negligibly small, and hence the formulated hopping model is adequate, only if  $g \ll 1$ .)

The dynamic Monte Carlo calculations were carried out using the algorithm suggested by Bakhvalov *et al* [18], which has become the *de facto* standard for the simulation of incoherent single-electron tunnelling [19]. All calculated variables were averaged over the sample, and in most cases over several (many) samples with independent random distributions

of localized sites in space and energy, but with the same dimensionless parameters  $L/a$ ,  $W/a$ ,  $T/T_0$ , and  $E/E_0$ . We have used a new, advanced technique [11] of noise (current spectral density) calculation to save simulation time. The supercomputer facilities used are listed in the acknowledgments section below.

### 3. DC current

In order to understand the relation between our model and the prior results in this field, we have started from the calculation of dc current  $\langle I \rangle$  as a function of  $T$  and  $E$ . If the electric field is sufficiently small ( $E \ll E_T$ ), then the current is proportional to  $E$ , and the transport is completely characterized by the linear conductivity  $\sigma \equiv \langle I \rangle / WE$ . Figure 1 shows the calculated conductivity as a function of temperature  $T$ . In the region  $T \ll T_0$  this dependence follows the exponential  $T$  dependence of the 2D Mott law [1–3]

$$\frac{\sigma}{\sigma_0} \approx A(T, 0) \exp \left[ - \left( B(T, 0) \frac{T_0}{T} \right)^{1/3} \right], \quad (5)$$

where  $A(T, E)$  and  $B(T, E)$  are dimensionless, model-dependent slow functions of their arguments. We have found that our results may be well fitted by equation (5) with the following pre-exponential function:  $A(T, 0) = (23.4 \pm 1.4)(T/T_0)^{(0.68 \pm 0.04)}$ , and constant  $B(T, 0) = 2.0 \pm 0.2$ .<sup>4</sup> This latter result may be compared with the following values reported in the literature. In [20],  $B$  was analytically estimated to be close to 2.1. A different value,  $3.45 \pm 0.2$ , has been found by mapping a random 2D hopping problem to the problem of percolation in a system of linked spheres [21, 2]. Finally, a close value 3.25 (with no uncertainty reported) has been obtained using numerical simulations of hopping on a periodic lattice, with a slightly different model for the function  $\Gamma(\Delta U)$  [22]. The difference between our result and the two last values is probably due to the differences between details of the used models.

At higher electric fields ( $E \gtrsim E_T$ ), dc current starts to grow faster than the Ohm law, so that if we still keep the above definition of conductivity  $\sigma$ , it starts to grow with  $E$  (figure 2). At  $T \rightarrow 0$ , the results are well described by the expression [23–27]

$$\frac{\sigma}{\sigma_0} \approx A(0, E) \exp \left[ - \left( B(0, E) \frac{E_0}{E} \right)^{1/3} \right]. \quad (6)$$

The data for not very high fields ( $E_T \ll E \ll E_0$ ) may be well fitted by equation (6) with constant  $B(0, E) = 0.65 \pm 0.02$  and pre-exponential function  $A(0, E) = (9.2 \pm 0.6)(E/E_0)^{(0.80 \pm 0.02)}$ . (Note that the value  $B(0, E) = 1.27$  given in [10] corresponds to a different pre-exponential function used for fitting.)

Finally, figure 2 shows that when the electric field becomes comparable with the value  $E_0$  defined by the second of equation (3), dc current, and hence conductivity, start to grow even faster than the exponential  $E$  dependence of equation (6).

### 4. Hopping statistics

In order to understand the physics of hopping in the three field regions better, it is useful to have a look at the statistics of localized site occupation and hopping length. We have found that

<sup>4</sup> In view of the approximate character of our model, in particular of equation (2), such accuracy may seem excessive, and for the purposes of comparison with actual physical experiments it certainly is. However, the accuracy is essential for the detection of Coulomb interaction effects in our following work [16], especially in the range of very high temperatures ( $T \sim T_0$ ) or fields ( $E \sim E_0$ ).

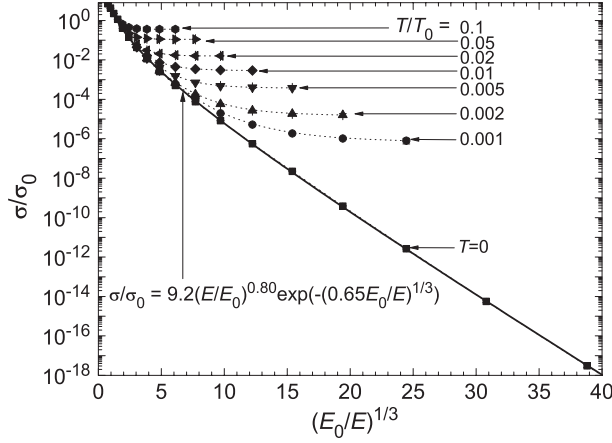


**Figure 2.** Nonlinear conductivity  $\sigma \equiv \langle I \rangle / WE$  as a function of electric field  $E$  for several values of temperature  $T$ . Each point represents data averaged over 80 samples of the same size, ranging from  $(20 \times 14)a^2$  to  $(1000 \times 700)a^2$ , depending on  $T$  and  $E$ . Points are Monte Carlo results. Thin dashed lines are only guides for the eye, while the thick solid line shows the best fit of the data by equation (6).

for all studied values of  $E$  and  $T$ , the probability of site occupation closely follows the Fermi distribution with the local Fermi level

$$\mu(\mathbf{r}) = \mu_L - e\mathbf{E}\mathbf{r} \quad (7)$$

(where  $\mu_L$  is the Fermi level of the source electrode) and some effective temperature  $T_{\text{eff}}$ . Points in figure 3 show  $T_{\text{eff}}$  as a function of electric field  $E$  for several values of physical temperature  $T$ . Dashed lines show the result of the best fitting of the naive single-particle master equation

$$\begin{aligned} \frac{\partial f(\epsilon, t)}{\partial t} = & \int d^2r \int d\epsilon' \exp\left(\frac{-r}{a}\right) \left\{ -\Gamma(\epsilon - \epsilon' + e\mathbf{E}\mathbf{r}) f(\epsilon) [1 - f(\epsilon')] \right. \\ & \left. + \Gamma(\epsilon' - \epsilon - e\mathbf{E}\mathbf{r}) f(\epsilon') [1 - f(\epsilon)] \right\} \end{aligned} \quad (8)$$

by a stationary Fermi distribution. Equation (8) would follow from our model if electron correlation (in particular, percolation) effects were not substantial. In reality, we can expect the results following from equation (8) to be valid only in certain limits<sup>5</sup>. For example, in the low field limit with  $E \rightarrow 0$ , both methods give  $T_{\text{eff}} = T$ . At higher fields the effective temperature grows with the applied field, which ‘overheats’ the electrons. At very high fields ( $E/E_0 \gtrsim 0.3$ ) both methods agree again and give

$$k_B T_{\text{eff}} \approx CeEa, \quad C = 0.71 \pm 0.02. \quad (9)$$

(A similar result, but with  $C \approx 1.34$ , for our definition of  $a$ , was obtained by Marianer and Shklovskii [28] for a rather different model with an exponential energy dependence of the density of states  $\nu_0$ .) However, at intermediate fields typical of ‘high-field’ variable-range hopping ( $E_T \ll E \ll E_0$ ), the master equation still gives the same result (9) and hence fails to appreciate that in fact  $T_{\text{eff}}$  is proportional to  $E^{2/3}$ .<sup>6</sup> In order to explain this result, let us discuss the statistics of hop lengths (figures 4 and 5).

<sup>5</sup> For a discussion of this issue, see section 4.2 of [2].

<sup>6</sup> In compensated semiconductors [2] with the number of hopping electrons (or holes) much smaller than the number of available hopping sites, the area of applicability of the master equation may be substantially broader. However, our model provides automatic half-filling of the available state band, and such filling evidently maximizes the electron correlation effects.

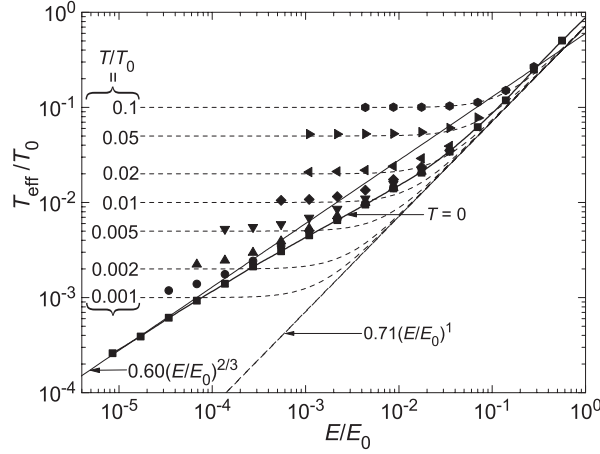


**Figure 3.** The effective temperature  $T_{\text{eff}}$  of current carriers as a function of electric field  $E$  for several values of temperature  $T$ . Closed points: Monte Carlo simulation results; dashed lines: master equation results. The solid curve marked  $T = 0$  is only a guide for the eye.

The two- and one-dimensional histograms in figure 4 show the probability density  $P$  of a hop between two sites separated by the vector  $\Delta \mathbf{r}$ , and also the density  $P_d$  weighted by the factor  $|H_{jk} - H_{kj}|$ , where each  $H$  is the total number of hops (during a certain time interval) in the indicated direction, i.e.  $jk \equiv j \rightarrow k$ . The latter weighting emphasizes the site pairs  $(j, k)$  contributing substantially to the net hopping transport, in comparison with ‘blinking’ pairs, which exchange an electron many times before allowing it to advance along the field. It is clear that at relatively high temperatures or low fields ( $E \ll E_T$ ) the non-weighted distribution should be symmetric (figure 4(a)). Figure 4(d) shows that in this case the one-dimensional probability density is well approximated by the Rayleigh distribution,  $P(r) \propto r \exp(-r/a_{\text{eff}})$ , with  $a_{\text{eff}} \approx a$ . However, the weighted hop distribution is strongly asymmetric even in the limit  $E \rightarrow 0$  (figure 4(b)). This asymmetry is even more evident at low temperatures or high fields ( $E \gg E_T$ ); in this case the distribution has a sharp boundary (figure 4(c)). Figure 4(d) shows those cases where the 1D histograms deviate substantially from the distribution predicted by the master equation—see the first of equations (16).

Figure 5 shows the rms non-weighted ( $r_{\text{rms}}$ ) and direction-weighted ( $r_{\text{rmds}}$ ) hop lengths, defined, respectively, as

$$r_{\text{rms}}^2 \equiv \frac{\sum_{j,k} r_{jk}^2 (H_{jk} + H_{kj})}{\sum_{j,k} (H_{jk} + H_{kj})} \quad (10)$$

and

$$r_{\text{rmds}}^2 \equiv \frac{\sum_{j,k} r_{jk}^2 |H_{jk} - H_{kj}|}{\sum_{j,k} |H_{jk} - H_{kj}|} \quad (11)$$

(that are of course just the averages of the histograms shown in figure 4), as functions of applied electric field for several values of temperature. At  $T \rightarrow 0$ , hopping is strictly one directional (i.e., if  $H_{jk} \neq 0$ , then  $H_{kj} = 0$ ), so that  $r_{\text{rms}}$  and  $r_{\text{rmds}}$  are equal. In fact, simulation shows that in this limit both lengths coincide, at lower fields following the scaling [23]

$$r_{\text{rms}} = r_{\text{rmds}} = Da \left( \frac{E_0}{E} \right)^{1/3}, \quad E_T \ll E \ll E_0, \quad (12)$$

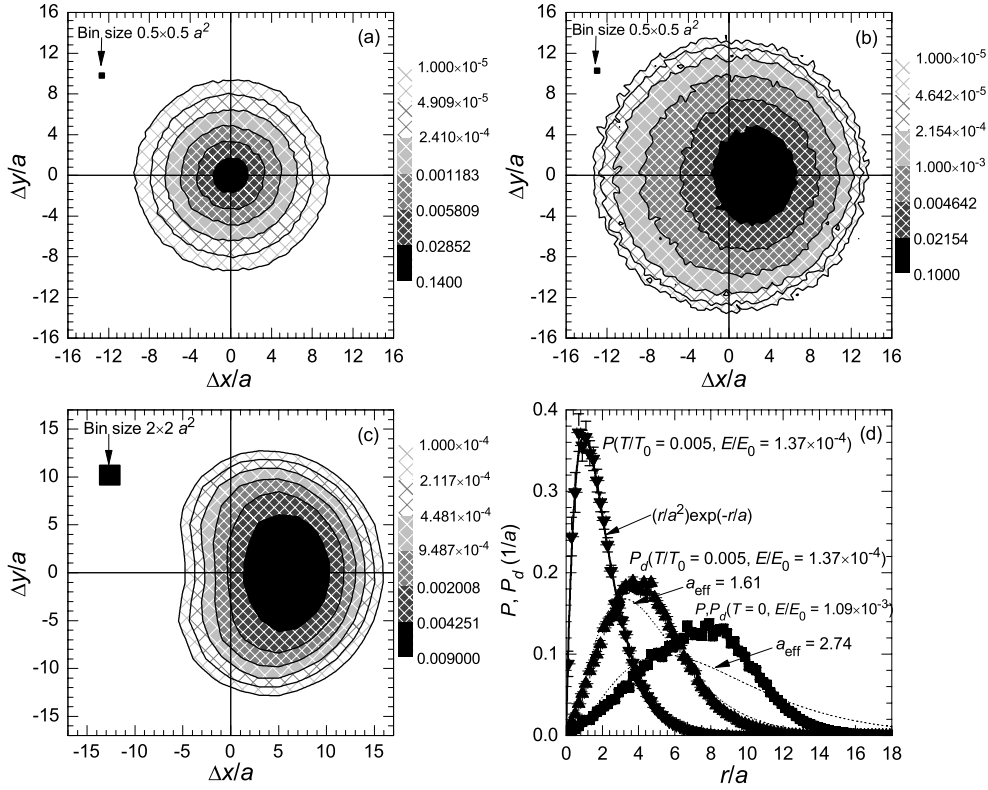


**Figure 4.** (a)–(c) Two-dimensional and (d) one-dimensional histograms of hop lengths for two typical cases: (a), (b)  $T/T_0 = 5 \times 10^{-3}$ ,  $E/E_0 = 1.37 \times 10^{-4}$  ( $E \ll E_T$ ) and (c)  $T = 0$ ,  $E/E_0 = 1.09 \times 10^{-3}$  ( $E_T \ll E$ ). The shade-coding in panels (a) and (c) corresponds to the probability  $P$  of hops with given  $\Delta \mathbf{r} = (\Delta x, \Delta y)$ , while that in panel (b) to the probability  $P_d$  weighted by the factor  $|H_{jk} - H_{kj}|$ —see the text. (Since at  $T = 0$  there are no backward hops, for the case shown in panel (c)  $P$  and  $P_d$  coincide.) Panel (d) shows  $P$  and  $P_d$ , averaged over all directions of vector  $\Delta \mathbf{r}$ , for the low-field, intermediate, and high-field cases. Dashed lines show the distribution (16) given by the master equation for the best-fit values of parameter  $a_{\text{eff}}$ .

with  $D = 0.72 \pm 0.01$ . (We are not aware of any prior results with which this value could be compared.)

This scaling of  $r$  in the variable-range hopping region is essentially the reason for the scaling of  $T_{\text{eff}}$  mentioned above; in fact, the hopping electron gas ‘overheating’ may be estimated by equating  $k_B T_{\text{eff}}$  to the energy gain  $eE \mathbf{r}_{\text{rms}}$ , possibly multiplied by a constant of the order of one. For the effective temperature, this estimate gives

$$k_B T_{\text{eff}} = \text{const} \times eE \mathbf{r}_{\text{rms}} = GeaE_0^{1/3} E^{2/3} = G \frac{(E/E_0)^{2/3}}{v_0 a^2}, \quad (13)$$

in accordance with the result shown in figure 3. Our Monte Carlo simulations give  $G = 0.60 \pm 0.02$ ; we are not aware of any previous results with which this number could be compared.

At higher fields ( $E \gtrsim 0.1E_0$ ) the hop lengths start to decrease more slowly, approaching a few localization lengths  $a$  (figure 5(a)). In this (‘ultra-high-field’) region, the energy range  $\sim eEa$  for tunnelling at distances of a few  $a$  is so high that there are always some accessible empty sites within this range, so that long hops, so dominant at variable-range hopping, do not contribute much to conduction.

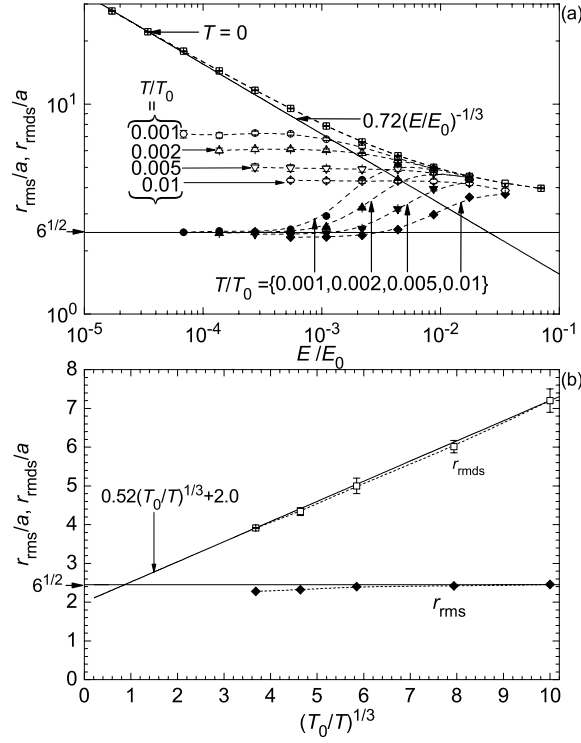


**Figure 5.** Rms hop length  $r_{\text{rms}}$  (solid points) and the weighted average hop length  $r_{\text{rmsd}}$  (open points) as functions (a) of applied electric field  $E$  for several temperatures  $T$ , and (b) of temperature at  $E \rightarrow 0$ . Tilted straight lines in panels (a) and (b) show the best fits by equation (12) and (17), respectively, while the horizontal thin lines show the values following from the master equation. Curves are only guides for the eye.

At finite temperatures, the most curious result is a non-monotonic dependence of the rms hopping length on the applied field—see figure 5(a). At  $E \rightarrow 0$ ,  $r_{\text{rms}}$  has to be field independent, and there is no scale for it besides  $a$ . (As evident as it may seem, this fact is sometimes missed in popular descriptions of hopping.) In order to make a crude estimate of  $r_{\text{rms}}$  in this limit, one can use the master equation (8). In this approach, at thermal equilibrium (i.e. at  $\Gamma$  independent of  $r$ ), the hop length probability density  $P(r)$  can be found as

$$P(r) = 2\pi r \int d\epsilon \int d\epsilon' \exp\left(\frac{-r}{a}\right) \left\{ \Gamma(\epsilon - \epsilon') f(\epsilon) [1 - f(\epsilon')] + \Gamma(\epsilon' - \epsilon) f(\epsilon') [1 - f(\epsilon)] \right\} \propto r \exp\left(\frac{-r}{a}\right), \quad (14)$$

in a good agreement with the results shown in figure 4(d) for this case. From equation (14), we get

$$r_{\text{rms}} \equiv \langle r^2 \rangle^{1/2} = \left[ \frac{\int P(r) r^2 dr}{\int P(r) dr} \right]^{1/2} = \sqrt{6}a \approx 2.45a, \quad (15)$$

in a good agreement with numerical data shown in figure 5.

A similar calculation for  $r_{\text{rms}}$  may be obtained by expanding the tunnelling rate  $\Gamma(\epsilon - \epsilon' + e\mathbf{E}\mathbf{r})$  in small electric field as  $\Gamma(\epsilon - \epsilon') + e\mathbf{E}\mathbf{r}\Gamma'(\epsilon - \epsilon')$ . The result is

$$P_d(r) = eEr^2 \int d\phi |\cos \phi| \int d\epsilon \int d\epsilon' \exp\left(\frac{-r}{a}\right) \times \{\Gamma'(\epsilon' - \epsilon) f(\epsilon') [1 - f(\epsilon)] + \Gamma'(\epsilon - \epsilon') f(\epsilon) [1 - f(\epsilon')]\},$$

$$P_d(r) \propto r^2 \exp\left(\frac{-r}{a}\right), \quad r_{\text{rms}} \equiv \left[ \frac{\int P_d(r) r^2 dr}{\int P_d(r) dr} \right]^{1/2} = \sqrt{12}a \approx 3.46a. \quad (16)$$

The Monte Carlo data (figure 5), however, differ from this result<sup>7</sup>, showing that at  $E \rightarrow 0$ ,  $r_{\text{rms}}$  obeys the Mott law [1–3]

$$r_{\text{rms}} = Ha \left(\frac{T_0}{T}\right)^{1/3} + Ia, \quad T \ll T_0, \quad (17)$$

with the best-fit values  $H = 0.52 \pm 0.05$  and  $I = 2.0 \pm 0.1$ . In contrast, the function  $r_{\text{rms}}(T)$  is rather far from equation (17), because the Mott law refers to long hops responsible for transport (with the average approximately corresponding to  $r_{\text{rms}}$ ), while  $r_{\text{rms}}$  reflects the statistics of all hops.

## 5. Shot noise

The current noise simulation has been limited to the case of zero temperature for two reasons. First, in the opposite limit ( $E_T \gg E$ ) current noise obeys the fluctuation–dissipation theorem; as a result, its low-frequency intensity can be found from  $\sigma(T)$ , and hence does not provide any new information. Second, the calculation of the spectral density  $S_I(f)$  of current fluctuations with acceptable accuracy requires a much larger statistical ensemble of random samples than that of the average current, which means it becomes increasingly difficult to extend it to finite temperatures even with the advanced averaging algorithm and substantial supercomputer resources used in this work.

Figure 6 shows a typical dependence of the current noise spectral density  $S_I$ , normalized to the Schottky value  $2e\langle I \rangle$ , on the observation frequency  $\omega \equiv 2\pi f$ . One can see a crossover from a low-frequency plateau to another plateau at high frequencies. As the sample length grows, the crossover becomes extended, i.e. features a broad intermediate range  $\omega_l \leq \omega \leq \omega_h$ , just like in 1D systems with next-site hopping [9]. The position of the high-frequency end  $\omega_h$  of this region can be estimated in the following way.

In all single-electron tunnelling systems, the high-frequency plateau is reached at frequency  $\omega_h$  close to the rate  $\Gamma$  of the fastest electron hops affecting the total current [9, 10, 29, 30]. (For example, in systems described by the ‘orthodox’ theory of single-electron tunnelling,  $\omega_h \approx \Gamma_{\text{max}} \approx \Delta U_{\text{max}}/e^2R \approx 1/RC$ , where  $R$  and  $C$  are, respectively, resistance and capacitance of a single junction [29, 30].) In our current case, this means that  $\omega_h \sim (\Gamma_{jk})_{\text{max}} \sim (g/\hbar)[\Delta U_{jk} \exp(-r_{jk}/a)]_{\text{max}}$ . For this estimate,  $\Delta U_{jk}$  can be taken as  $k_B T_{\text{eff}}$  from figure 3, while according to the histograms shown in figure 4(d) the length of shortest hops, still giving a noticeable contribution to the current, can be estimated as  $\sim r_{\text{rms}}/2$ . For the case shown in figure 6 ( $E/E_0 = 8.75 \times 10^{-3}$ ), these estimates yield  $\Delta U_{jk}/k_B T_0 \approx 2 \times 10^{-2}$ ,  $(r_{jk})_{\text{min}}/a \approx 2.5$ , giving finally  $\omega_h/\omega_0 \sim 1.5 \times 10^{-3}$ , in a very reasonable agreement with numerical results shown in figure 6. (Note that this simple estimate, giving a length-independent value for  $\omega_h$ , is only valid for relatively long and broad samples.)

<sup>7</sup> This result emphasizes again that the validity of the master equation approach is very limited, and for most transport characteristics this equation fails to give quantitatively correct results for any region in the  $[E, T]$  space.

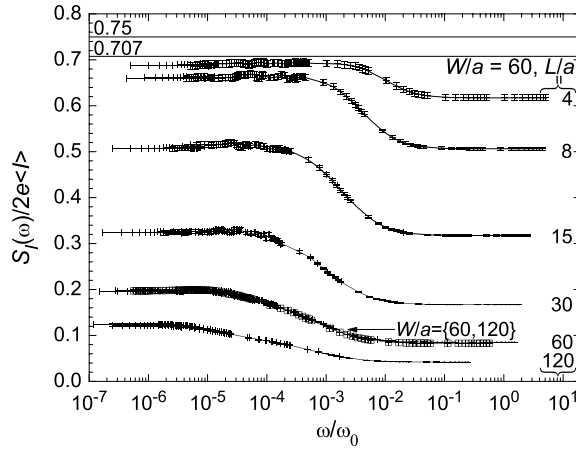


**Figure 6.** Spectral density  $S_I$  of current fluctuations normalized to the Schottky noise  $2e\langle I \rangle$  as a function of observation frequency  $\omega$ , measured in units of  $\omega_0 \equiv g/\hbar v_0 a^2$ , for several values of sample length  $L$  for  $T = 0$  and  $E/E_0 = 8.75 \times 10^{-3}$ . Small points show results for  $W/a = 60$ , while open squares are for  $W/a = 120$  (at  $L/a = 60$ ). Horizontal lines correspond to the Fano factor for hopping through short samples with one and two localized sites [7, 8]. Curves are only guides for the eye.

At  $\omega \rightarrow 0$ , a crossover to  $1/f$  noise might be expected, because the discussion of this effect in some earlier publications [31, 32] was apparently independent of the Coulomb interaction between hopping electrons. However, within the accuracy of our simulations, we could not find any trace of  $1/f$ -type noise for any parameters we have explored. This fact may not be very surprising, because all the discussions of the  $1/f$  noise we are aware of require the presence of thermal fluctuations which are absent in our case ( $T = 0$ ).

Since the low-frequency spectral density is flat, at  $T = 0$  it may be considered as shot noise<sup>8</sup> and characterized by the Fano factor [4]

$$F \equiv \frac{S_I(f \rightarrow 0)}{2e\langle I \rangle}. \quad (18)$$

Similarly, in order to characterize the flat high-frequency spectral density, we may use the parameter

$$F_\infty \equiv \frac{S_I(f \rightarrow \infty)}{2e\langle I \rangle}. \quad (19)$$

Figure 7(a) shows the average Fano factors  $F$  and  $F_\infty$  as a function of  $L$  for several values of the applied electric field, while figure 7(b) shows that the same data can be collapsed on universal curves by the introduction of certain length scales:  $L_c$  for  $F$  and  $L_h$  for  $F_\infty$ .

For the high frequency case,

$$F_\infty = \left( \frac{L_h}{L} \right)^\beta, \quad L \gg L_h, \quad (20)$$

where, within the accuracy of our calculations,  $\beta = 1$ . Such dependence could be expected, because the high-frequency noise at hopping can be interpreted as a result of the ‘capacitive

<sup>8</sup> In the case of hopping, the noise intensity is not exactly proportional to dc current, because the noise suppression factor depends on the ratio  $L/L_c$ , where the characteristic length  $L_c$  is itself a function of applied electric field, and hence (implicitly) of dc current—see figures 7, 8 and their discussion below.

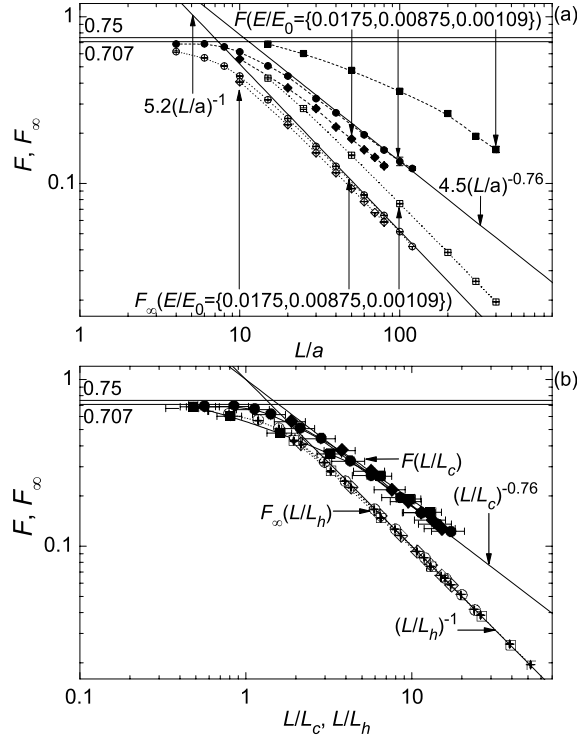


**Figure 7.** Average Fano factor  $F$  and its high-frequency counterpart  $F_\infty$  as functions of sample length  $L$  normalized to (a) the localization length  $a$ , and (b) the scaling lengths  $L_c$  (for  $F$ ) and  $L_h$  (for  $F_\infty$ ) (see figure 8 below), for several values of applied field at  $T = 0$  and  $W \gg L_c$ . Horizontal lines correspond to the average Fano factor for hopping via one and two localized sites [7, 8]. Straight lines are the best fits to the data, while dashed curves are only guides for the eye.

division' of the discrete increments of externally measured charge jumps resulting from single-electron hops through the system [6]. When applied to uniform (ordered) systems, these arguments always give the result  $F_\infty \approx 1/N_h$  with  $N_h = L/d$  being the number of electron hops ( $d$  the hopping length along the current flow) necessary to pass an electron through the system, regardless of hop rates [4, 5, 9]. For  $T \rightarrow 0$  in the case of disordered conductors,  $L_h$  in equation (20) may then be interpreted as the average hop length along current flow. This interpretation turns out to be correct. Indeed, figure 8 shows that the parameter  $L_h$  obtained from equation (20) scales with the electric field in a manner similar to  $x_{\text{rms}}$ , especially at low fields, where it follows the variable-range hopping dependence of equation (12).

The low-frequency value  $F$ , in the limit ( $L \ll L_c$ ), is weakly dependent on length and approaches  $F \approx 0.7$ , which not surprisingly is consistent with the prior results for hopping via one intermediate site [7] ( $F = 0.75$ ) and two such sites [8] ( $F = 0.707$ ). The results for long samples are much more interesting. We have found that they may be reasonably well fitted with a universal dependence

$$F = \left(\frac{L_c}{L}\right)^\alpha, \quad L \gg L_c. \quad (21)$$

Here  $\alpha$  is a numerical exponent; in the current study we could establish that

$$\alpha = 0.76 \pm 0.08. \quad (22)$$

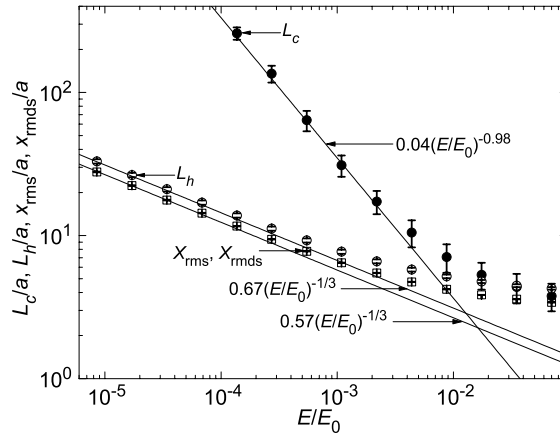


**Figure 8.** The values of  $L_h$  and  $L_c$  giving the best fitting of shot noise results by equations (20) and (21) as functions of applied electric field  $E$  (open and solid circles, respectively). Open squares show the simple and direction-weighted average hop length along the applied field direction, defined similarly to equations (10) and (11). Straight lines are the best fits to the data.

Equation (21) and the value for  $\alpha$  are compatible with our previous results [10]  $\alpha = 0.85 \pm 0.07$  (for the same model, but just one particular value of  $E$ ) and  $\alpha = 0.85 \pm 0.02$  (for nearest neighbour hopping on uniform slanted lattices).

Figure 8 shows the fitting parameter  $L_c$  as a function of electric field  $E$ . In the variable-range hopping region, it may be fitted with the following law:

$$L_c = Ja \left( \frac{E_0}{E} \right)^\mu, \quad J = 0.04 \pm 0.01, \quad \mu = 0.98 \pm 0.08. \quad (23)$$

This law may be compared with the result of the following arguments. According to the arguments given in [10], parameter  $L_c$  may be interpreted as the average percolation cluster length (up to a constant of the order of unity). The theory of directed percolation [33–35] gives the following scaling:

$$L_c \propto \langle x \rangle \left( \frac{x_c}{|\langle x \rangle - x_c|} \right)^{\delta_{\parallel}}. \quad (24)$$

Here  $\langle x \rangle$  is the rms hop length along the field direction, while  $x_c$  is its critical value. According to [35], the critical index  $\delta_{\parallel}$  should be close to 1.73. Due to the exponential nature of the percolation,  $|\langle x \rangle - x_c| \sim a$ , while  $\langle x \rangle$  should follow a field scaling similar to that given by equation (12). (Square points in figure 8 show that this is true for our simulation results as well.) Thus for sufficiently large  $\langle x \rangle$  we arrive at equation (23) with  $\mu = \frac{1}{3}(1 + \delta_{\parallel}) \approx 0.911$ . Equation (24) shows that this value is quite compatible with our numerical result, thus confirming the interpretation of  $L_c$  as the average percolation cluster length.

Note that in the variable-range hopping regime,  $L_c$  has a different field dependence and is much larger than the average hop length. However, as the applied electric field approaches  $E_0$ , both lengths become comparable with each other and with the localization radius  $a$ .

## 6. Discussion

To summarize, our results for average conductivity and hop statistics are in agreement with the well known semi-quantitative picture of hopping, including the usual variable-range hopping at

low fields ( $E \ll E_T$ ) and ‘high-field’ variable-range hopping at  $E_T \ll E \ll E_0$ . However, our supercomputer-based simulation has allowed, for the first time, a high-precision quantitative characterization of hopping, for a particular but very natural model. Moreover, our model also describes the ‘ultra-high field’ region ( $E \sim E_0$ ) where the variable-range hopping picture is no longer valid, since from most localized sites an electron can hop, with comparable probability, to several close sites. (In the last region, there are no clearly defined percolation clusters; rather, electrons follow a large number of interwoven trajectories.)

Our simulations of shot noise in 2D hopping have confirmed our earlier hypothesis [10] that in the absence of substantial Coulomb interaction, in sufficiently large samples ( $L, W \gg L_c$ ), the Fano factor  $F$  scales approximately proportionally to  $1/L$ —see equation (21). Other confirmations of this hypothesis have come from recent experiments with lateral transport in SiGe quantum wells [36] and GaAs MESFET channels [37, 38]. Unfortunately, these experiments are not precise enough to distinguish the small difference between the exponent  $\alpha$  in equation (21) and unity.

The hypothesis that  $\alpha$  is in fact equal to unity for sufficiently long samples seems appealing, because it would mean the simple addition of mutually independent noise voltages generated by sample sections connected in series. In contrast, a deviation of  $\alpha$  from unity would mean that some dynamic correlations of electron motion persist even at  $L \gg L_c$ . For 1D hopping this fact is well established: in at least one exactly solvable model (the ‘asymmetric single exclusion process’, or ASEP [39]) the dynamic correlations may change  $\alpha$  from 1 to 0.5. However, for 2D conductors the fact that the correlation length (if any) may be substantially larger than the percolation cluster length comes as a surprise<sup>9</sup>.

From the point of view of possible applications in single-electron devices [15], the fact that  $F$  may be suppressed to values much less than unity is generally encouraging, since it enables the use of circuit components with quasi-continuous charge transport. However, in order to achieve the high-quality quasi-continuous transfer (say,  $F \lesssim 0.1$ ), the sample length  $L$  has to be at least an order of magnitude longer than the percolation cluster length scale  $L_c$ . On the other hand,  $L_c$  itself, especially in the most interesting case of low applied fields, is substantially longer than the localization length  $a$  (figure 8), which is of the order of a few nanometres in most prospective materials, e.g., amorphous silicon. Hence, it may be hard to implement sub-electron transport in conductors substantially shorter than  $\sim 100$  nm. This size is quite acceptable for experiments at low temperatures (say, below 1 K), but is too large for the most important case of room-temperature single-electron circuits [15], because of large stray capacitance of the hopping conductor, which effectively sums up with the capacitance of the island to be serviced.

## Acknowledgments

Fruitful discussions with A Efros, V Kozub, M Pollak, B Shklovskii and D Tsigankov are gratefully acknowledged. The work was supported in part by the Engineering Physics Program of the Office of Basic Energy Sciences at the US Department of Energy. We also acknowledge the use of the following supercomputer resources: our group’s cluster *Njal* (purchase and installation funded by DoD’s DURIP programme via AFOSR), Oak Ridge National Laboratory’s IBM SP computer *Eagle* (funded by the Department of Energy’s Office of Science and Energy Efficiency Program), and also the IBM SP system Tempest at Maui High Performance Computing Center and the IBM SP system Habu at NAVO Shared Resource

<sup>9</sup> Our calculation methods are hardly a suspect, since they give  $\alpha \approx 1$  for substantial Coulomb interaction [16], and also the similar  $1/L$  law for high-frequency fluctuations (both with or without Coulomb interaction).

Center. Computer time on the two last machines has been granted by the DOD's High Performance Computing Modernization Program.

## References

- [1] Mott N F and Davies J H 1979 *Electronic Properties of Non-Crystalline Materials* 2nd edn (Oxford: Oxford University Press)
- Mott N F 1993 *Conduction in Non-Crystalline Materials* 2nd edn (Oxford: Clarendon)
- [2] Shklovskii B I and Efros A L 1984 *Electronic Properties of Doped Semiconductors* (Berlin: Springer)
- [3] Efros A L and Pollak M (ed) 1991 *Hopping Transport in Solids* (Amsterdam: Elsevier)
- [4] Blanter Ya and Buttiker M 2000 *Phys. Rep.* **336** 2
- [5] Matsuoka K A and Likharev K K 1998 *Phys. Rev. B* **57** 15613
- [6] Averin D V and Likharev K K 1991 *Mesoscopic Phenomena in Solids* ed B L Altshuler, P A Lee and R A Webb (Amsterdam: Elsevier) p 173
- [7] Nazarov Yu V and Struben J J R 1996 *Phys. Rev. B* **53** 15466
- [8] Kinkhabwala Y and Korotkov A N 2000 *Phys. Rev. B* **62** R7727
- [9] Korotkov A N and Likharev K K 2000 *Phys. Rev. B* **61** 15975
- [10] Sverdlov V A, Korotkov A N and Likharev K K 2001 *Phys. Rev. B* **63** 081302(R)
- [11] Sverdlov V A, Kinkhabwala Y A and Korotkov A N 2005 *Preprint cond-mat/0504208*
- [12] Nguen V L, Spivak B Z and Shklovskii B I 1985 *Sov. Phys.—JETP* **62** 1021
- [13] Medina E, Kardar M, Shapir Y and Wang X R 1989 *Phys. Rev. Lett.* **62** 941
- [14] Wang X R, Shapir Y, Medina E and Kardar M 1990 *Phys. Rev. B* **42** 4559
- [15] Likharev K 1999 *Proc. IEEE* **87** 606
- [16] Kinkhabwala Y A, Sverdlov V A and Likharev K K 2006 *J. Phys.: Condens. Matter* **18** 2013  
(Kinkhabwala Y A, Sverdlov V A and Likharev K K 2004 *Preprint cond-mat/0412209*)
- [17] Sameshita T and Usui S 1991 *J. Appl. Phys.* **70** 1281
- [18] Bakhvalov N S, Kazacha G S, Likharev K K and Serdyukova S I 1989 *Sov. Phys.—JETP* **68** 581
- [19] Wasshuber C 2001 *Computational Single-Electronics* (Berlin: Springer) chapter 3
- [20] Brenig W, Döhler G H and Heyszenau H 1973 *Phil. Mag.* **27** 1093
- [21] Skal A S and Shklovskii B I 1974 *Fiz. Tverd. Tela.* **16** 1820  
Skal A S and Shklovskii B I 1974 *Sov. Phys.—Solid State* **16** 1190 (Engl. Transl.)
- [22] Tsigankov D N and Efros A L 2002 *Phys. Rev. Lett.* **88** 176602
- [23] Shklovskii B I 1972 *Fiz. Tekh. Poluprov.* **6** 2335  
Shklovskii B I 1973 *Sov. Phys.—Semicond.* **6** 1964 (Engl. Transl.)
- [24] Apsley N and Hughes H P 1974 *Phil. Mag.* **30** 963  
Apsley N and Hughes H P 1975 *Phil. Mag.* **31** 1327
- [25] Pollack M and Riess I 1976 *J. Phys.: Condens. Matter* **9** 2339
- [26] Rentzsch R, Shlimak I S and Berger H 1979 *Phys. Status Solidi a* **54** 487
- [27] van der Meer M, Schuchardt R and Keiper R 1982 *Phys. Status Solidi b* **110** 571
- [28] Marianer S and Shklovskii B I 1992 *Phys. Rev. B* **46** 13100
- [29] Korotkov A N, Averin D V, Likharev K K and Vasenko S A 1992 *Single-Electron Tunneling and Mesoscopic Devices* ed H Koch and H Luebbig (Berlin: Springer) p 45
- [30] Korotkov A N 1994 *Phys. Rev. B* **49** 10381
- [31] Shklovskii B I 1980 *Solid State Commun.* **33** 273  
Kogan Sh M and Shklovskii B I 1981 *Sov. Phys.—Semicond.* **15** 605
- [32] Shklovskii B I 2003 *Phys. Rev. B* **67** 045201
- [33] Stauffer D and Aharony A 1994 *Introduction to Percolation Theory* Revised 2nd edn (Philadelphia: Taylor and Francis)
- [34] Obukhov S P 1980 *Physica A* **101** 145
- [35] Essam J W, De'Bell K, Adler J and Bhatti F M 1986 *Phys. Rev. B* **33** 1982
- [36] Kuznetsov V V, Mendez E E, Zuo X, Snider G and Croke E 2000 *Phys. Rev. Lett.* **85** 397
- [37] Roshko S H, Safonov S S, Savchenko A K, Tribe W R and Linfield E H 2002 *Physica E* **12** 861
- [38] Savchenko A K, Safonov S S, Roshko S H, Bagrets D A, Jouravlev O N, Nazarov Y V, Linfield E H and Ritchie D A 2004 *Phys. Status Solidi b* **241** 26–32
- [39] Derrida B 1998 *Phys. Rep.* **301** 65